Supporting Information

Unlocking catalytic potential of single-atom Zn on N-doped MXene through intensive metal-support interaction for high-efficiency Fenton-like catalysis

Chunyu Zhang[a#], Huanran Ma[b#], Xiufang Zhang[a], Jiliang Ma[a*], Guanlong Wang[a*]

[a]School of Light Industry and Chemical Engineering, Dalian Polytechnic University, Dalian 116034, China

[b]College of Environmental Science and Engineering, Dalian Maritime University, Dalian 116026, China

[*]Corresponding author: Guanlong Wang; E-mail: wanggl@dlpu.edu.cn

Jiliang Ma; E-mail: jlma@dlpu.edu.cn

[#]Co-first authors: These authors contributed equally to this work

Table of Content

Text S1. Chemicals and materials

Aluminium titanium carbide (Ti_3AlC_2, 400 mesh) was purchased from Foshan

Xinen Technology, Guangdong Province, China; lithium fluoride (LiF, 99.9%), zinc chloride ($ZnCl_2$), tetracycline (TC), 4-chlorophenol (4-CP), humic acid (HA), tert-butanol (TBA), atrazine (ATZ), methyl phenyl sulfoxide (PMSO), methyl phenyl sulfone ($PMSO_2$) and methyl methylene sulfoxide (DMSO) were purchased from Shanghai McLean Biochemical Technology Co. Ltd. Carbon nanotubes (>97% purity) were procured from Shenzhen Nano Technology Co., Ltd. Hydrochloric acid (HCl), urea ($CO(NH_2)_2$), sodium thiosulfate ($Na_2S_2O_3$), phenol (PE), potassium dihydrogen phosphate (KH_2PO_4), sodium hydroxide (NaOH), sodium bicarbonate ($NaHCO_3$), sodium chloride (NaCl), p-benzoquinone (ρ-BQ), methanol (MeOH), furfuryl alcohol (FFA), benzoic acid (BA), nitrobenzene (NB) and sodium sulfate (Na_2SO_4) were purchased from Tianjin Komeo Chemical Reagent Co., Ltd; sulfamethoxazole (SMX), potassium thiocyanate (KSCN), potassium peroxymonosulfate (Oxone, $KHSO_5$-$0.5KHSO_4$-$0.5K_2SO_4$) and potassium iodide (KI) were purchased from Aladdin Reagent (Shanghai) Co. Ltd. Bisphenol A (BPA) was purchased from Tianjin Damao Chemical Reagent Factory. All reagents were analytically pure and the water was ultrapure water (resistivity > 18 MΩ cm).

Text S2. Characterizations

Scanning electron microscope (SEM) (Hitachi, accelerating voltage 20 kV) was

used to characterize the morphology of MXene and different Zn-N-MXene. The element composition of MXene, Zn-N-MXene-3 and Zn-N-CNT was determined using energy dispersive spectrometer (EDS, JSM-7800F). Aberration-corrected high-angle annular dark-field scanning transmission electron microscopy (AC-HAADF-STEM, American FEI Spectra 300) was used to probe the single-atom Zn distribution on Zn-N-MXene-3. The crystal structure of different Zn-N-MXene was detected by X-ray diffraction (XRD, Shimadzu LabX-6100) (λ = 1.5418 Å). The Zn, N, Ti, C and O species on Zn-N-MXene-3 and N-MXene were determined using X-ray photoelectron spectroscopy (XPS, scalab250 spectrometer). The interaction between PMS and Zn-N-MXene-3 and Zn-N-CNT was determined using in-situ Raman spectroscopy (Raman, Japan Horiba LabRAM HR Evolution). The reducibility of Zn-N-MXene-3 and Zn-N-CNT was determined by hydrogen temperature-programmed reduction (H_2-TPR) on a programmed temperature-raising chemisorption analyzer (Priority 5080). The reactive species in Zn-N-MXene-3/PMS and Zn-N-CNT/PMS systems were detected by an electron paramagnetic resonance spectrometer (EPR, Bruker EMXplus-6/1), with 5, 5-Dimethyl-1-pyrroline-N-oxide (DMPO) and 2, 2, 6, 6-tetramethylpiperidine (TEMP) as spin-trapping reagents. The Zn loading amount of Zn-N-MXene-3 and Zn-N-CNT, and metal leaching were measured by inductively coupled plasma-atomic emission spectroscopy (ICP-OES, American Agilent 5110). The open-circuit voltage (OCP), cyclic voltammetry (CV), electrochemical impedance spectra (EIS), linear sweep voltammetry (LSV) and Tafel slope tests were carried out using an electrochemical workstation (Shanghai Tatsunghwa

Instrumentation Co., Ltd., CHI-660D).

Text S3. Synthesis of MXene and Zn-N-MXene/PVDF membrane

1) Synthesis of MXene

Firstly, an etching solution was prepared by mixing 9 M HCl and 2 g LiF in 30 mL of solution. Next, 0.8 g Ti_3AlC_2 was gradually added to this solution. The resulting suspension was stirred at 45 °C for 24 h to allow complete reaction. The mixture was then centrifuged at 7000 rpm for 10 min, and the supernatant was discarded. The product was washed four times with 2 M HCl, followed by repeated washing with ultrapure water until the pH of supernatant reached neutrality. The clay-like precipitate obtained was placed in a flask with 100 mL ultrapure water and sonicated under a nitrogen atmosphere for 1 h. Finally, after centrifugation at 7000 rpm for 10 min and vacuum freeze-drying for 48 h, oligolayered MXene nanosheets were obtained. The specific reaction equations are shown in **Eqs. S1-S2**.

$$LiF + HCl \rightarrow LiCl + HF \quad (S1)$$

$$Ti_2AlC_3 + HF \rightarrow AlF_3 + Ti_2C_3 + H_2 \quad (S2)$$

2) Synthesis of Zn-N-MXene/PVDF membrane

18 mg of Zn-N-MXene material was ultrasonically dispersed in 36 mL of ethanol to obtain a homogeneous Zn-N-MXene dispersion with a concentration of 0.5 mg mL^{-1}. Subsequently, the Zn-N-MXene dispersion was filtered onto a PVDF membrane support via vacuum filtration (1 bar vacuum pressure) to prepare a Zn-N-MXene/PVDF membrane.

Text S4. Analytic methods

The concentrations of PE, BPA, 4-CP, TC, SMX and ATZ during the reaction

were determined by HPLC. The specific analysis methods were as follows:

The mobile phases for PE, BPA, 4-CP and ATZ were methanol and ultrapure water in the ratio of 7:3 at a detection wavelength of 271, 276, 280 and 214 nm, respectively. The mobile phase for TC was acetonitrile and phosphate buffer (pH = 7.3) in the ratio of 7:3 at a detection wavelength of 358 nm. The mobile phase for SMX was 7:3 acetonitrile and 0.1% acetic acid at a detection wavelength of 270 nm. The above flow rates were all 1 mL min^{-1}.

The mineralization degree of pollutants was determined by a total organic carbon analyzer (TOC, Shimadzu TOC-L CPH, Japan).

Text S5. The calculation and quantification methods

(1) The kinetic constant (k) is the reaction rate calculated using a pseudo-first-order

kinetic model:

$$\ln(C/C_0) = -kt \quad \text{(S3)}$$

In this case, C_0 is the initial organic pollutant concentration and C is the organic pollutant concentration at different times; *k* is the kinetic constant; and t is the reaction time.

(2) The turnover frequency (TOF, min^{-1})

$$TOF = \frac{\Delta n}{(m \times \omega \times t)/M} \quad \text{(S4)}$$

In this case, Δn is the moles of converted pollutants, mol; m is the mass dosage of catalyst, g; ω is the mass fraction of Zn in the catalysts, wt%; t is the reaction time, min; M is the atomic weight of Zn, g mol^{-1}.

(3) Quantification method for PMS concentration

The mixture containing 0.5 mol L^{-1} KI and 0.05 mol L^{-1} $NaHCO_3$ was prepared. Subsequently, 0.1 mL of the sample was thoroughly blended with 4.9 mL of the prepared solution. Following a 20 min reaction period, the absorbance of the sample was measured using a UV-vis spectrophotometer (INESA-L5) at a wavelength of 352 nm.

(4) The steady-state concentration and contribution of ROSs:

The concentrations of the probe compounds BA (1 μM), NB (1 μM) and FFA (5 μM) were chosen at the level that did not affect SMX degradation, and the steady-state concentrations and contribution ratio of •OH, $SO_4^{\bullet-}$ and $^1O_2$ can be calculated by the following equations:

$$-\frac{\mathrm{d}[\mathrm{BA}]}{\mathrm{d}t} = k_{\mathrm{BA},\cdot\mathrm{OH}}\left[\cdot\mathrm{OH}\right][\mathrm{BA}] + k_{\mathrm{BA},\mathrm{SO}_4^{\cdot-}}\left[\mathrm{SO}_4^{\cdot-}\right][\mathrm{BA}] \quad \text{(S5)}$$

$$-\frac{\mathrm{d}[\mathrm{NB}]}{\mathrm{d}t} = k_{\mathrm{NB},\cdot\mathrm{OH}}\left[\cdot\mathrm{OH}\right][\mathrm{NB}] \quad \text{(S6)}$$

$$-\frac{\mathrm{d}[\mathrm{FFA}]}{\mathrm{d}t} = k_{\mathrm{FFA},\cdot\mathrm{OH}}\left[\cdot\mathrm{OH}\right][\mathrm{FFA}] + k_{\mathrm{FFA},{}^1\mathrm{O}_2}\left[{}^1\mathrm{O}_2\right][\mathrm{FFA}] \quad \text{(S7)}$$

$[\cdot\mathrm{OH}]_{ss}$, $[\mathrm{SO}_4^{\cdot-}]_{ss}$ and $\left[{}^1\mathrm{O}_2\right]_{ss}$ can then be obtained:

$$\left[\cdot\mathrm{OH}\right]_{ss} = \frac{k_{\mathrm{NB}}}{k_{\mathrm{NB},\cdot\mathrm{OH}}} \quad \text{(S8)}$$

$$\left[\mathrm{SO}_4^{\cdot-}\right]_{ss} = \frac{k_{\mathrm{BA}} - \left[\cdot\mathrm{OH}\right]_{ss} k_{\mathrm{BA},\cdot\mathrm{OH}}}{k_{\mathrm{BA},\mathrm{SO}_4^{\cdot-}}} \quad \text{(S9)}$$

$$\left[{}^1\mathrm{O}_2\right]_{ss} = \frac{k_{\mathrm{FFA}} - \left[\cdot\mathrm{OH}\right]_{ss} \times k_{\mathrm{FFA},\cdot\mathrm{OH}}}{k_{\mathrm{FFA},{}^1\mathrm{O}_2}} \quad \text{(S10)}$$

$$k_{SMX} = (k_{SMX,\cdot\mathrm{OH}}\left[\cdot\mathrm{OH}\right]_{ss} + k_{SMX,\mathrm{SO}_4^{\cdot-}}\left[\mathrm{SO}_4^{\cdot-}\right]_{ss} + k_{SMX,{}^1\mathrm{O}_2}\left[{}^1\mathrm{O}_2\right]_{ss}) \quad \text{(S11)}$$

$$Contribution\ (\%) = \frac{[ROS]_{ss} \times k_{SMX,ROS}}{k_{SMX}} \quad \text{(S12)}$$

$k_{NB,^{\bullet}OH}$ (3.9×10^9 M^{-1} s^{-1}), $k_{BA,^{\bullet}OH}$ (5.9×10^9 M^{-1} s^{-1}) and $k_{BA,SO_4^{\bullet-}}$ (1.2×10^9 M^{-1} s^{-1}) are the second-order rate constant of •OH with NB and •OH and $SO_4^{\bullet-}$ with BA respectively. $k_{FFA,^{\bullet}OH}$ (3.6×10^9 M^{-1} s^{-1}), $k_{FFA,^1O_2}$ (1.2×10^8 M^{-1} s^{-1}) and $k_{FFA,PMS}$ (0.011 M^{-1} s^{-1})[1] are the second-order rate constants of $^{\bullet}OH$ and $^1O_2$ with FFA, respectively. $k_{SMX,^{\bullet}OH}$ (6.78×10^9 M^{-1} s^{-1}), $k_{SMX,SO_4^{\bullet-}}$ (0.93×10^8 M^{-1} s^{-1}) and $k_{SMX,^1O_2}$ (0.011 M^{-1} s^{-1})[2] are the second-order rate constants of $SO_4^{\bullet-}$, $^{\bullet}OH$ and $^1O_2$ with SMX, respectively.

Text S6. Electrochemical test methods

The conventional three-electrode system was used to perform electrochemical tests, including OCP, EIS, CV, LSV and Tafel slope. The working electrode, counter electrode and reference electrode were a glassy carbon electrode loaded with Zn-N-MXene, a platinum wire electrode and a saturated calomel electrode, respectively. 2.5 mg of Zn-N-MXene was dispersed in a mixture of 985 μL of ultrapure water and 15 μL of Nafion solution, which was sonicated to make the dispersion uniform. 10 μL of the above mixture was added dropwise to the glassy carbon electrode and left to dry naturally before use. Experiments were carried out using 0.1 M Na_2SO_4 aqueous

solution as the electrolyte, and 0.65 mM PMS and 0.1 mM SMX were added to the electrolyte if necessary.

Text S7. DFT calculation methods

The DFT calculations were carried out using the Vienna Ab-initio Simulation Package (VASP)[3, 4] with the frozen-core all-electron projector-augment-wave (PAW)[5, 6] method. The Perdew-Burke-Ernzerhof (PBE)[7] of generalized gradient approximation (GGA) was adopted to describe the exchange and correlation potential. The cutoff energy for the plane-wave basis set was set to 450 eV. A 5-layer 4×4 Zn (002) slab was used, and a vacuum region of 15 Å above it was used to ensure the decoupling between neighboring systems. The geometry optimizations were performed until the forces on each ion was reduced below 0.02 eV/Å, and a Gamma 1×1×1 Monkhorst-

Pack k-point[8] sampling of the Brillouin zone was used. The DFT-D3 method was used to describe the van der Waals interaction.[9]

Zn-N-MXene-3 and Zn-N-CNT was calculated using a Gaussian smearing method and a width of 0.05 eV allowing for partial occupation of the Kohn-Sham orbital. The electronic energy was considered self-consistent when the energy change was smaller than 10- 5 eV. A geometry optimization was considered convergent when the force change was smaller than 0.05 eV/Å. Grimme's DFT-D3 methodology was used to describe the dispersion interactions.[10] The vacuum spacing perpendicular to the plane of the structure is 20 Å. The Brillouin zone integral utilized the surfaces structures of 2×2×1 monkhorst pack K-point sampling. Finally, the adsorption energies (E_{ads}) were calculated as $E_{ads} = E_{ad/sub} - E_{ad} - E_{sub}$, where $E_{ad/sub}$, E_{ad}, and E_{sub} are the total energies of the optimized adsorbate/substrate system, the adsorbate in the structure, and the clean substrate, respectively.

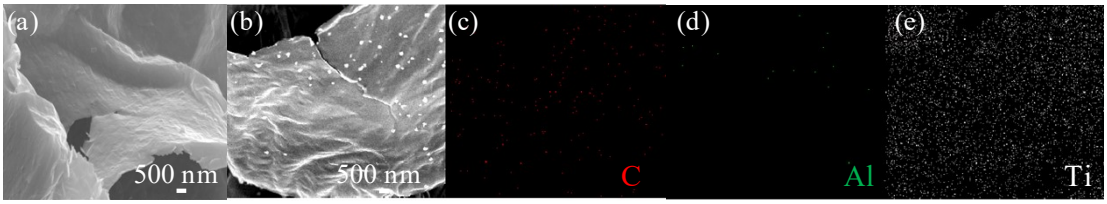

Fig. S1. (a-b) SEM images of MXene; (c-e) EDS mapping images of Ti, C, and Al elements on MXene.

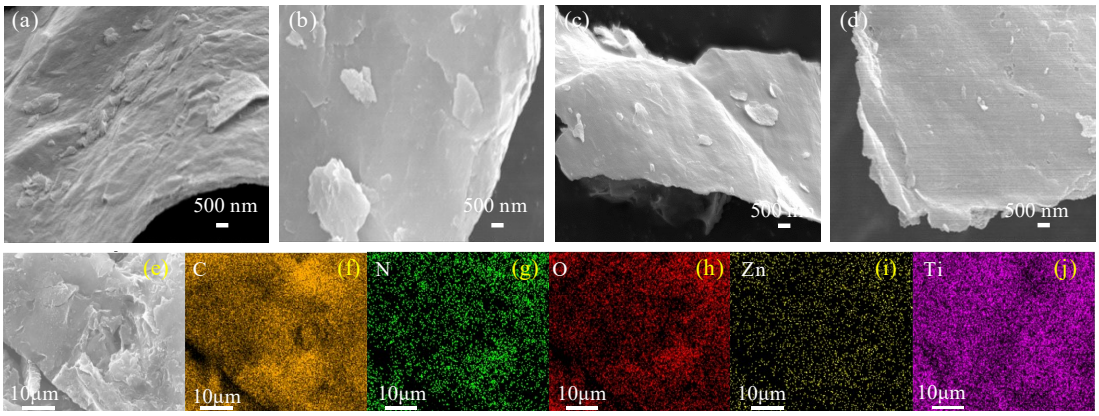

Fig. S2. SEM images of Zn-N-MXene-1 (a), Zn-N-MXene-2 (b), Zn-N-MXene-3 (c) and Zn-N-MXene-4 (d); (e-j) EDS mapping images of C, N, O, Zn and Ti elements on Zn-N-MXene-3.

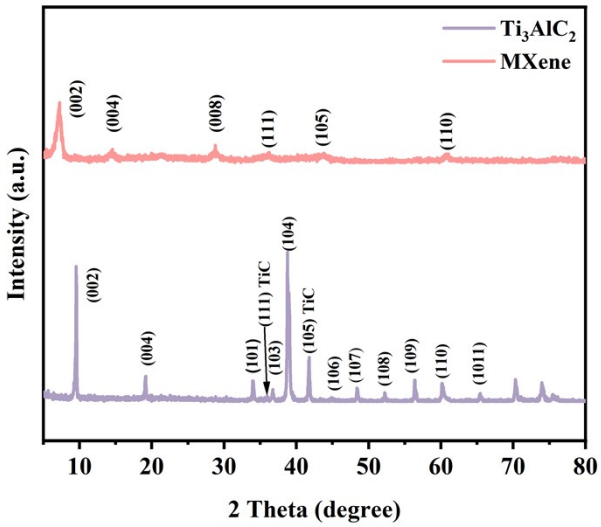

Fig. S3. XRD patterns of Ti_3AlC_2 and $Ti_3C_2T_x$ MXene.

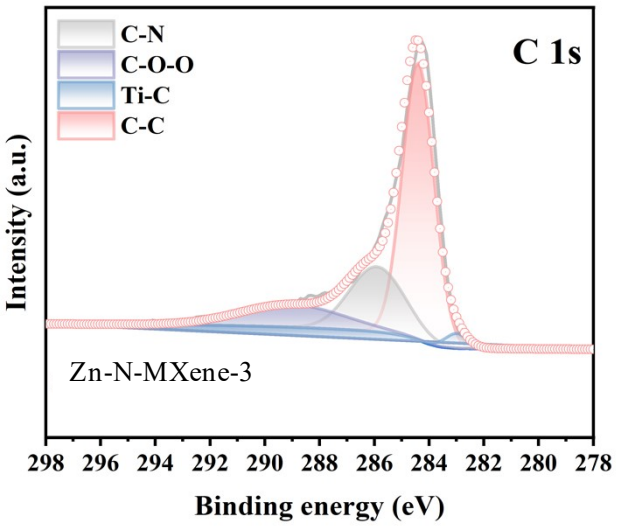

Fig. S4. High-resolution XPS spectra of C 1s for Zn-N-MXene-3.

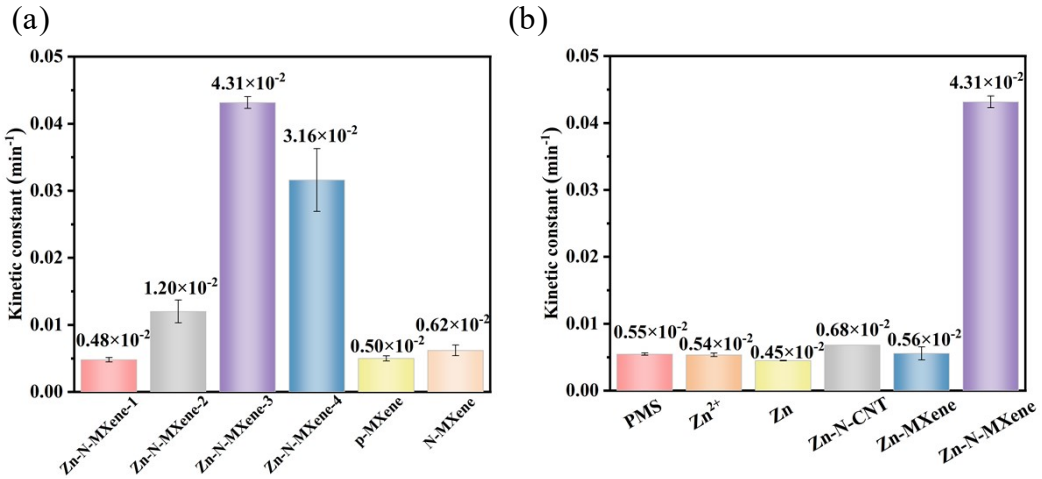

Fig. S5. Kinetic constants of SMX degradation on (a) different Zn-N-MXene and (b) PMS and different Zn-based catalysts.

.

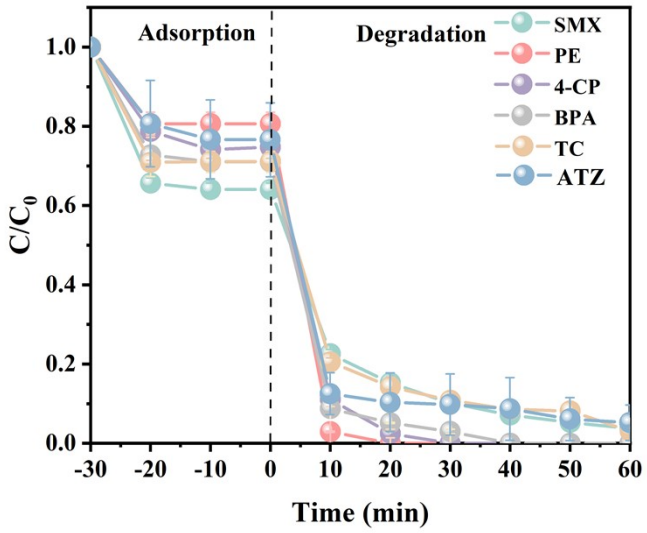

Fig. S6. Performance of Zn-N-MXene-3/PMS in removing various pollutants. ($[Pollutant]_0$ = 0.1 mM, [Catalyst] = 0.03 g L^{-1}, [PMS] = 0.65 mM, pH_0 = 5.3).

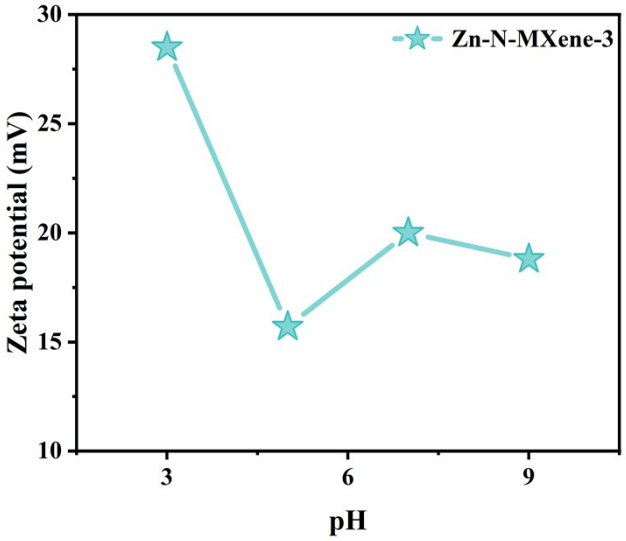

Fig. S7. Zeta potential of Zn-N-MXene-3 at different pH.

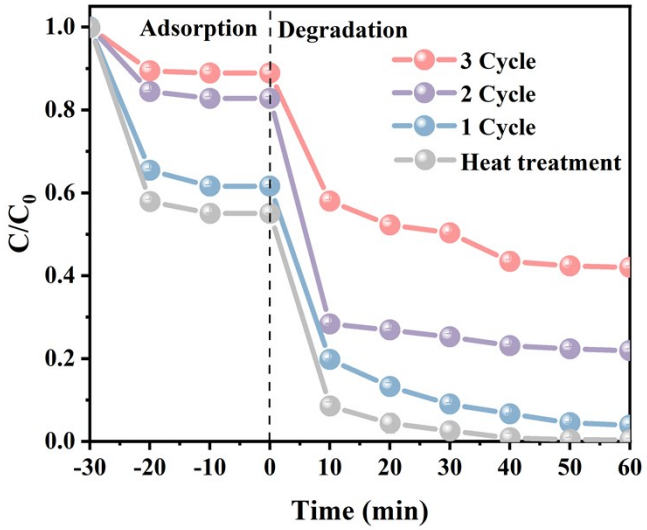

Fig. S8. Cyclic and regeneration experiment of Zn-N-MXene-3/PMS. ($[SMX]_0$ = 0.1 mM, [Catalyst] = 0.03 g L^{-1}, [PMS] = 0.65 mM).

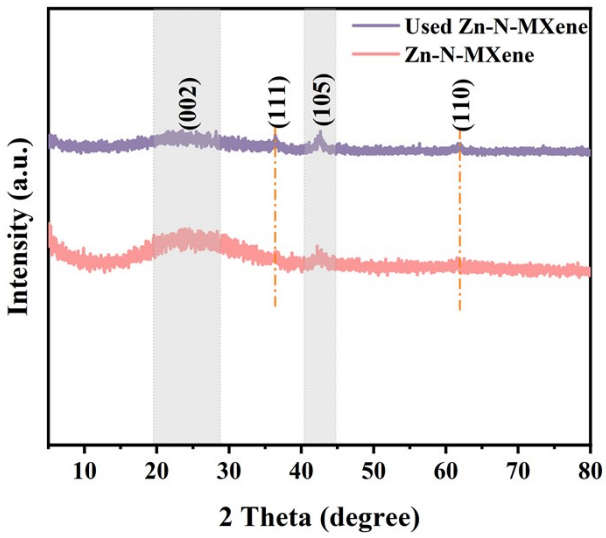

Fig. S9. XRD patterns of Zn-N-MXene-3 before and after reaction.

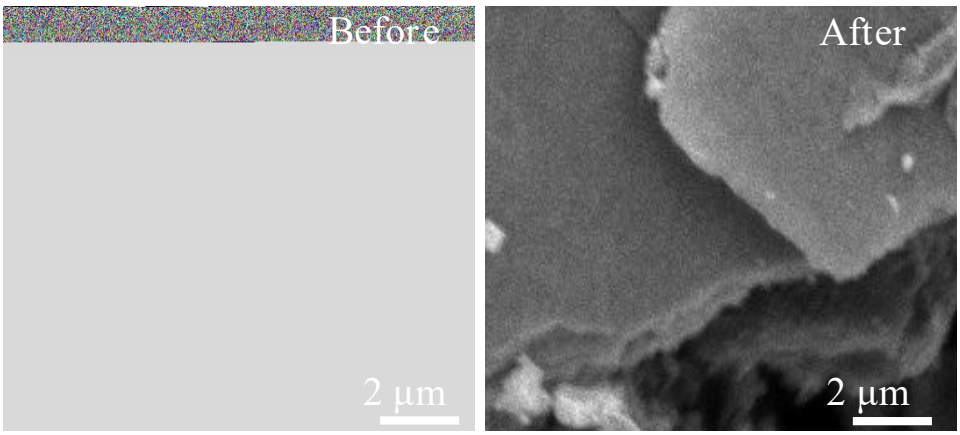

Fig. S10. SEM images of Zn-N-MXene-3 before and after reaction.

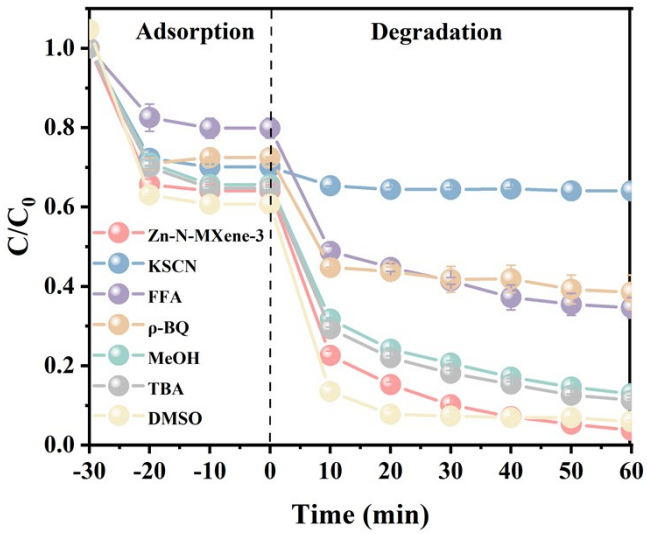

Fig. S11. SMX removal by Zn-N-MXene-3/PMS system in the presence of different trapping agents.

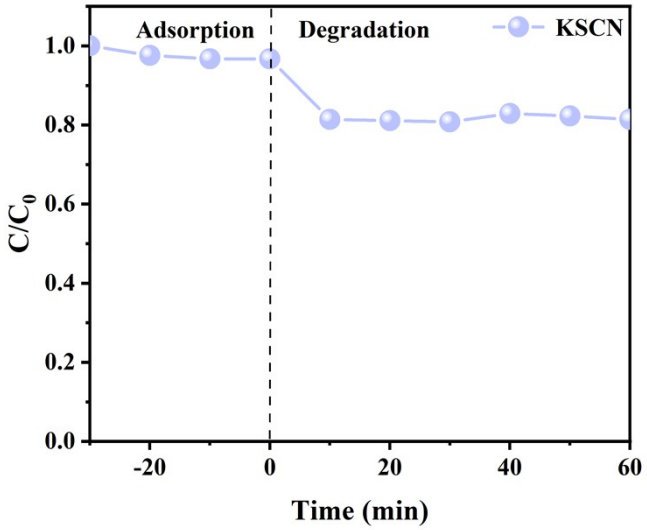

Fig. S12. SMX removal by Zn-N-MXene-3/PMS system in the presence of KSCN.

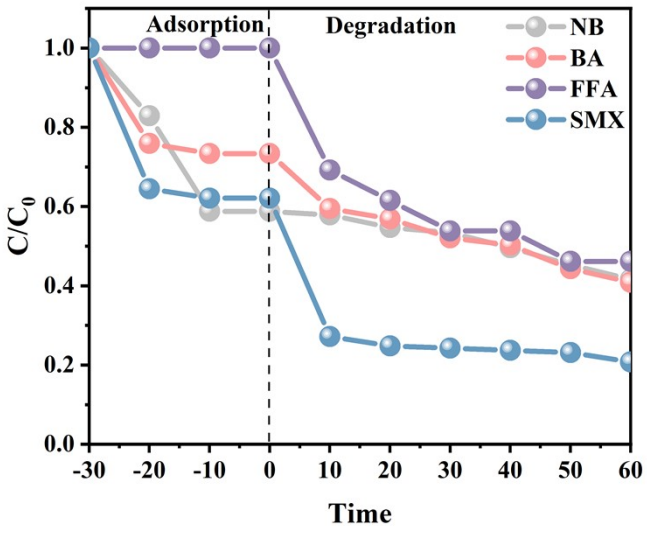

Fig. S13. The performance of Zn-N-MXene-3/PMS system for NB, BA, FFA and SMX removal in competitive kinetics experiments. ($[BA]_0 = [NB]_0$ = 1 μL, $[FFA]_0$ = 5 μL, $[SMX]_0$ = 0.1 mM, [Catalyst] = 0.03 g L^{-1}, [PMS] = 0.65 mM, pH_0 = 7).

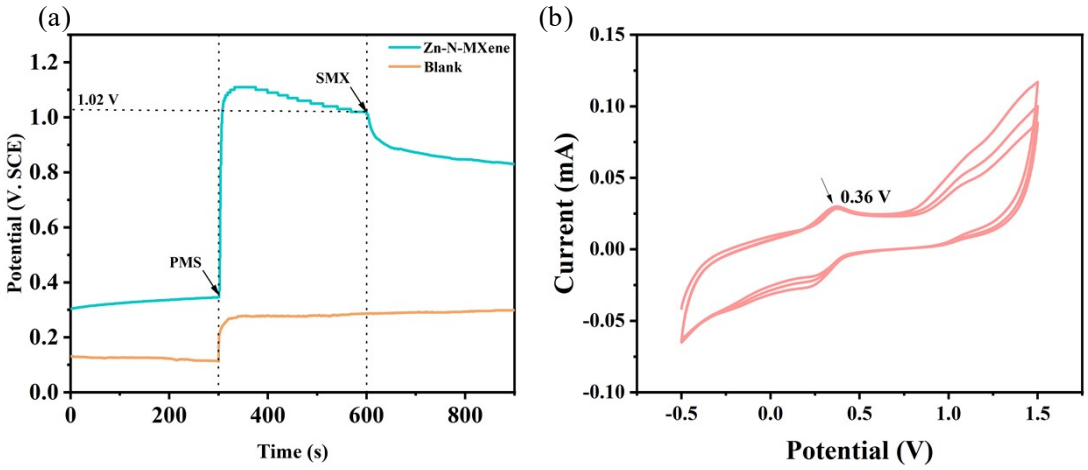

Fig. S14. (a) OCP profiles of Zn-N-MXene-3 after addition of PMS and SMX; (b) CV curves of Zn-N-MXene-3 in the presence of SMX.

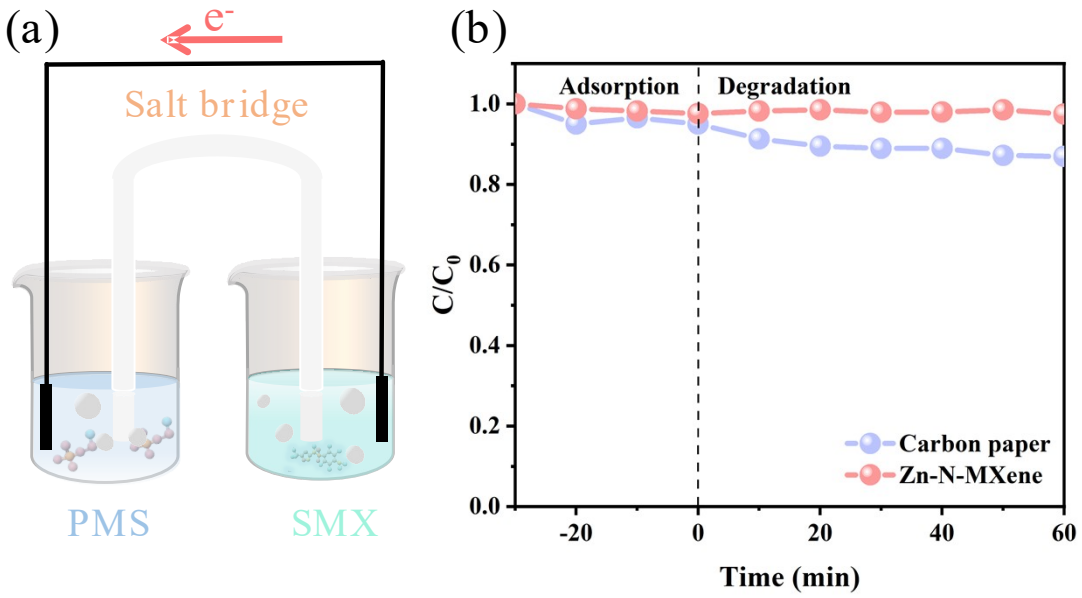

Fig. S15. (a) Schematic diagram of galvanic oxidation system; (b) SMX degradation in different GOS.

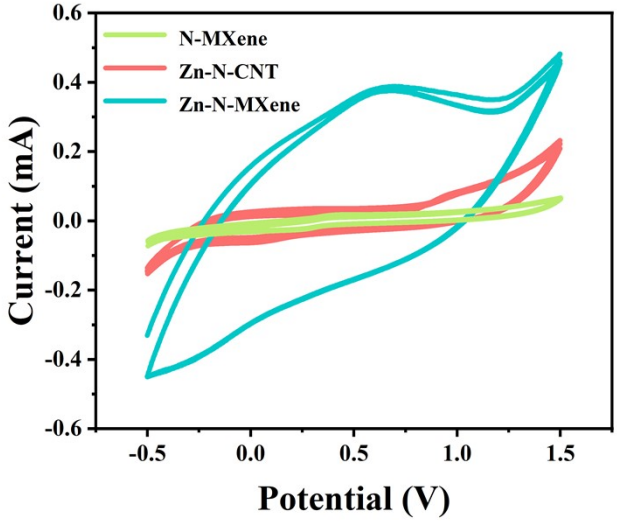

Fig. S16. CV curves of N-MXene, Zn-N-CNT and Zn-N-MXene-3.

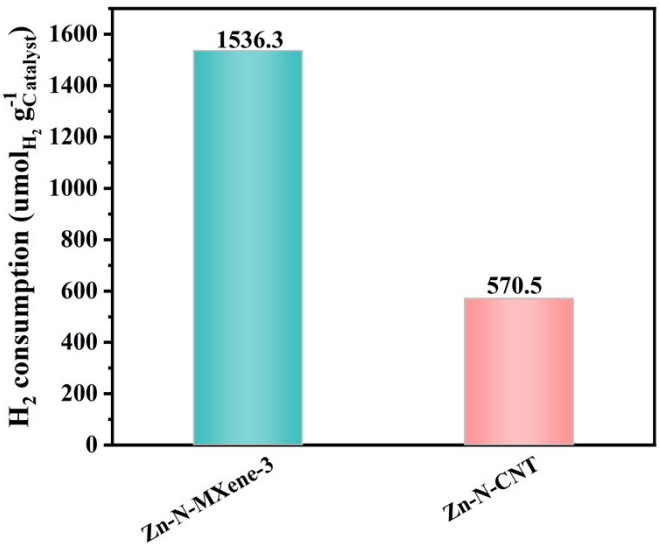

Fig. S17. H_2 consumption of Zn-N-MXene-3 and Zn-N-CNT.

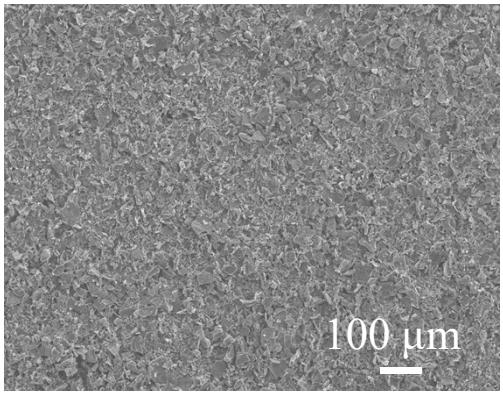

Fig. S18. SEM image of Zn-N-MXene-3/PVDF membrane surface.

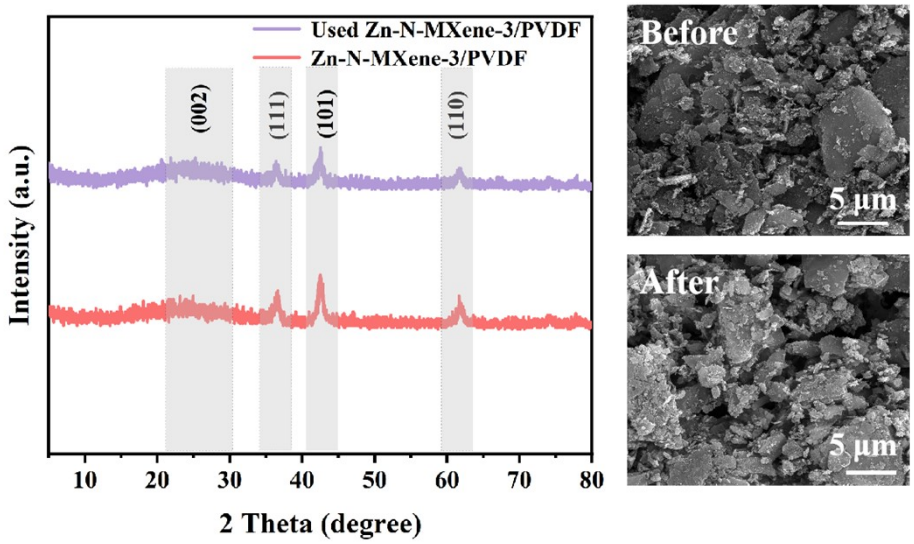

Fig. S19. XRD patterns and SEM images of Zn-N-MXene-3/PVDF membrane before and after reaction.

Table S1. The element composition of MXene.

Elemental	Ti	Al	C
Content (wt %)	92.79	0.33	6.88

Table S2. The element composition of Zn-N-MXene-3.

Element	Atomic Fraction (%)	Atomic Error (%)	Mass Fraction (%)	Mass Error (%)	Fit Error (%)
C	87.18	1.46	80.94	1.78	1.09
N	4.94	1.01	5.35	1.09	7.77
O	6.28	1.19	7.77	1.45	2.63
Ti	1.58	0.27	5.84	0.95	2.62
Zn	0.02	0.02	0.10	0.12	120.03

Table S3. Element composition determined by XPS for different Zn-N-MXene samples (at %).

	Zn-N-MXene-1	Zn-N-MXene-2	Zn-N-MXene-3	Zn-N-MXene-4	N-MXene
Zn	0.19	0.21	0.18	0.26	/
N	7.95	7.01	7.98	7.82	6.97
C	22.59	43.71	60.09	66.63	42.18
O	29.50	25.95	19.86	16.80	13.53
Ti	39.77	23.13	11.89	8.49	37.32

Table S4. The metal content derived from ICP-OES, SMX removal efficiency and reaction rate constant on different catalysts.

	Sample	Metal content (wt %)	Removal efficiency (%)	k (min^{-1})
1	Zn-N-MXene-3	0.11	97	0.0430
2	Zn-N-CNT	0.18	40	0.0068

Table S5 Performance comparison between Zn-N-MXene-3 and reported single-atom catalysts.

	Catalyst (dosage, g L^{-1})	Metal content (wt %)	Removal efficiency (%)	k (min^{-1})	TOF (min^{-1})	Pollutant (mM)	PMS (mM)	Ref.
1	Zn-N-MXene-3 (0.03)	0.11	96.3 (60 min)	0.0430	3.16	SMX (0.10)	0.65	This work
2	Zn-N-MXene-3 (0.03)	0.11	100 (20 min)	0.332	9.85	PE (0.10)	0.65	This work
3	SA-Zn-NC (0.10)	0.28	98 (30 min)	0.136	0.379	AO7 (0.050)	0.20	[11]
4	Cu_{SA}/CN P&S (0.05)	0.62	100 (4.5 min)	1.51	2.06	BPA (0.045)	0.50	[12]
5	FeNC-edge (0.02)	0.74	100 (8 min)	1.15	0.473	BPA (0.010)	1.0	[13]
6	Fe-N/Cl-C (1.00)	0.20	100 (30 min)	0.138	0.0411	ACV (0.044)	3.0	[14]
7	Co-N_2 (0.20)	2.40	100 (5 min)	0.695	0.123	BPA (0.050)	2.0	[15]
8	Fe-N_4-C_6O_2 (0.10)	2.63	100 (30 s)	13.3	2.13	BPA (0.050)	0.40	[16]
9	Zn-N@C (0.05)	0.36	95.7 (20 min)	0.190	0.432	SMX (0.025)	0.50	[17]
10	Fe-N_3O_1 (0.10)	5.49	100 (20 min)	0.472	0.0204	SMX (0.040)	1.0	[18]
11	Co_1CNCl/S (0.05)	1.43	100 (5 min)	0.952	1.80	PE (0.20)	0.40	[19]

Table S6. Leaching content of Zn and Ti in reaction process (mg L^{-1}).

Element	Zn	Ti
Content (mg L^{-1})	0.0018	0.0176

Table S7. The contribution ratios of reactive species in Zn-N-MXene-3/PMS systems (%).

Catalyst	•OH	$SO_4^{\bullet-}$	$^1O_2$	SMET
Zn-N-MXene-3	77.56%	0.41%	17.38%	4.65%

Table S8. Utilization ratio of PMS for Zn-N-MXene and Zn-N-CNT (%).

Catalyst	PMS (mM)	Consumption ratio of PMS	SMX (%)	SMX (mM)	•OH (mM)	Utilization ratio of PMS (%)[20]
Zn-N-MXene-3/PMS	0.65	49.5%	96.3	0.1	0.0963	29.93
Zn-N-CNT/PMS	0.65	42.0%	40	0.1	0.04	14.65

•OH yield (equal to PMS consumption): $N = n \times \omega$, where n is the total mole quantity of SMX, ω is the SMX removal efficiency.

Total PMS consumption: $N_1 = n_{1\times}\omega_1$, where n is the total mole quantity of PMS, ω is the consumption ratio of PMS.

Utilization ratio of PMS: U = PMS consumption/Total PMS consumption = N/N_1

Table S9. The water quality parameters of surface water.

Parameters	Value
pH	7.08
UV254 (A)	0.11
COD (mg L^{-1})	75.63

TOC (mg L^{-1})	8.15

References

1 L. W. Gao, Y. Guo, J. H. Zhan, G. Yu, Y. J. Wang, *Water Res.*, 2022, 221, 118730.

2 X. N. Hu, M. S. Zhu, *Environ. Sci. Technol.*, 2024, 58, 10415-10444.

3 G. Kresse, J. Hafner, *Phys. Rev. B*, 1994, 49, 14251-14269.

4 G. Kresse, J. Furthmüller, *Phys. Rev. B*, 1996, 54, 11169-11186.

5 P. E. Blöchl, *Phys. Rev. B* 1994, 50, 17953-17979.

6 G. Kresse, D. Joubert, *Phys. Rev. B*, 1999, 59, 1758-1775.

7 B. Hammer, L. B. Hansen, J. K. Nørskov, *Phys. Rev. B*, 1999, 59, 7413-7421.

8 H. J. Monkhorst, J. D. Pack, *Phys. Rev. B*, 1976, 13, 5188-5192.

9 S. Grimme, J. Antony, S. Ehrlich, H. Krieg, *J. Chem. Phys.*, 2010, 132.

10 G. Henkelman, B. P. Uberuaga, H. Jónsson, *J. Chem. Phys.*, 2000, 113, 9901-9904.

11 Z. Y. Zhao, H. B. Tan, P. Zhang, X. Y. Liang, T. Li, Y. W. Gao, C. Hu, *Angew. Chem., Int. Ed.*, 2023, 135, e202219178.

12 Y. Shen, Y. L. Pan, C. Zhu, H. Z. Zhang, J. Wang, R. L. Liu, Q. L. Fang, S. Song, B. L. Chen, *Small*, 2024, 20, 2406319.

13 D. Lee, J.Lee, G. Yu, K. Kim, J. Kim, D. H. Mok, A. Jang, M. Jung, H. Ahn, S. Back, T. Hyeon, C. Lee, *Small*, 2025, 21, 2408811.

14 S. Y. Ren, Y. T. Wang, L. Shi, X. Xu, S. Zhong, K. S. Hu, H. Y. Zhou, Z. S. Zhu, P. Zhou, W. J. Tian, J. Zuo, J. B. Yi, X. H. Guan, X. G. Duan, S. B. Wang, *Adv. Mater.*, 2025, 37, 2415339.

15 X. Y.;Liang, D. Wang, Z. Y. Zhao, T. Li, Y. W. Gao, C. Hu, *Adv. Funct. Mater.*, 2022, 32, 2203001.

16 T. T. Chen, G. B. Zhang, H. W. Sun, Y. T. Hua, S. Yang, D. D. Zhou, H. X. Di, Y. L. Xiong, S. H. Hou, H. Xu, L. Z. Zhang, *Nat. Commun.*, 2025, 16, 2402.

17 Y. N. Xiao, J. H. Hu, X. Y. Li, Y. B. Zou, Y. Li, L. Lin, B. Li, *Chem. Eng. J.*, 2023, 474, 145973.

18 Y. X. Zeng, J. Deng, N. Zhou, W. Xia, Z. H. Wang, B. Song, Z. W. Wang, Y. Yang, X. Xu, G. M. Zeng, C. Y. Zhou, *Small*, 2024, 20, 2311552.

19 Z. S. Zhu, Y. T. Wang, P. T. Wang, S. Zhong, K. S. Hu, S. Y. Ren, J.P. Vongsvivut, H.Q. Sun, X.G. Duan, S.B. Wang, *Nat. Water*, 2025, 3, 211-221.

20 Q. L. Jiang, Y. K. Ma, P. X. Zhao, X. S. Li, Y. T. Shao, X. M. Xu, *Environ. Sci. Technol.*, 2025, 59, 14182-14192.